PREPARATION AND SURFACE PROPERTIES OF AMPHIPHILIC GREEN MAGNETITE NANOPARTICLES CAPPED WITH BRANCHED IONIC LIQUID

A. M. ATTA[a, b*], H. A. AL-LOHEDAN[a], A. O. EZZAT[a], A. M. TAWFIK[c]
[a]*Department of Chemistry, College of Science, King Saud University, Riyadh 11451, Saudi Arabia*
[b]*Petroleum application department, Egyptian petroleum research institute, Nasr city 11727, Cairo, Egypt.*
[c]*College of Science, King Saud University, Riyadh, Saudi Arabia*

Magnetite nanoparticles (MNPs) have an excellent electrochemical behaviors in aqueous medium having several industrial applications. New quaternized ionic liquids derivatives, namely octahydroxyethylamino pentaertheritoltetrapropanoate p-toluene sulfonate (OATPS) is synthesized to use as capping agent for MNPs to increase their dispersability and chemical stability to inhibit the corrosion of steel in aqueous acid solution. The chemical structure of OATPS is elucidated from NMR analyses. Electrochemical behaviors of magnetite coated with OATPS in acid chloride solution have been investigated to determine its corrosion inhibition efficiency (IE%). Different concentrations of both capped magnetite and OATPS concentrations are ranged from 1 to 150 ppm were used to study the effect of concentrations on its adsorption at steel surfaces in acid chloride aqueous solution. The electrochemical measurements indicate that the OATPS IL and capped magnetite behave as mixed-type corrosion inhibitors. Moreover, the adsorption process of OATPS IL obeys the Langmuir adsorption isotherm at steel/water interface. The electrochemical techniques showed agreements for determining IE% of magnetite capped OATPS IL for steel in acid chloride solution.

(Received March 24, 2016; Accepted May 13, 2016)

Keywords: Steel; EIS; inhibition; hyperbranched; ionic liquid; surface properties

1. Introduction

Mild steel is widely used in the production, transportation and storage of petroleum crude oil and gas [1]. The oilfield equipment suffer from corrosion of corrosive down hole and surfaces environments especially that caused by corrosion in acidic environments [2]. Amphiphilic ionic liquids (ILs) have received considerable attention recently as potential "green" alternate to surfactants to apply in the field of petroleum fields such as demulsifiers and corrosion inhibitors [1-5]. These compounds showed great capability to adsorb at interfaces and to improve the surface wetting characteristics [5]. Moreover, ILs possess good surface properties and have ability to form micelle with the formation of segregates are formed [6] which increased capability to apply as corrosion inhibitors in acidic media [7, 8]. It is well established that the adsorption of corrosion inhibitors on steel increase the corrosion-resistance behavior of steel [8]. Moreover, it was also reported that the ILs have been used in oil fields to minimize the corrosion of steel produced from carbon dioxide and hydrogen sulfide [9, 10]. Commercial ILs used as corrosion inhibitors are based on organic cation (i.e. piperidinium, pyridinium, phosphonium, etc.) in combination with a complex anion (i.e halides, cyanide, etc.) [11-13]. It was also previously reported that the dendrimers possess superior properties that can be applied in several industries [14-16].

* Corresponding author: khaled_00atta@yahoo.com

Magnetite nanoparticles are finding increasing applications in the electrochemistry and corrosion protection of steel [17-20]. The magnetite nanomaterials have great tendency to form aggregates and it is quite challenging to disperse in aqueous medium and tend to dissolve in acidic medium. The capping agents based on natural products, polymers, dendrimers, surfactants and ionic liquids attracted great attention to apply as stabilizer for inorganic nanoparticles [21-24]. Poly (ionic liquids), PILs, are also known as ‘‘polyelectrolytes’’ have been widely used as excellent capping agents for different types of colloidal dispersions of metal nanoparticles [25-27]. Recently we have synthesized different types of PILs as nanoparticles have excellent electrochemical characteristics [28-30]. Encouraged by the excellent performance of dendrimers as scale inhibitors and anticorrosive coatings, we succeeded to prepare dendritic ester amine derivatives with properly designed structures might also be used as efficient water soluble corrosion [31]. It was found that a significant advantage to apply dendrimers to form well adhered anticorrosive films. As far as we are aware, the hyperbranched ionic liquid has not been reported previously in the literature. For this reason, the present work, the preparation of amphiphilic ionic liquid based on petaerythretol to combine properties of surfactants, polymers and dendrimer is the main objective of the present work to apply as stabilizer for magnetite nanoparticles. The effect of ionic liquid on the stability and size of nanoparticles based on magnetite will be investigated in this work.

2. Experimental

2.1 Materials

Ferric chloride hexahydrate, potassium iodide, diethanolamine (DEA), p-toluene sulfonic acid (PTSA), pentaerythritol tetracrylate (PETA) and ammonium hydroxide (25 wt %)were produced from Aldrich Chemical Co. Steel having composition (wt %): 0.14% C, 0.57% Mn, 0.21% P, 0.15% S, 0.37% Si, 0.06% V, 0.03% Ni, 0.03% Cr and Fe balance is used to measure its corrosion efficiencies in 1 M aqueous HCl solution.

2.2 Synthesis technique

a)The synthesis of amine ester monomer

Tetrakis, N,N-diethylol-3-amine pentaerthritol ethanoate monomer was prepared by reacting PETA and DEA via Michael addition reaction. In this respect, pentaerythritol tetracrylate (0.1 mol) and diethanolamine (0.4 mol) were mixed with methanol solvent 100 mL) at 35 ^{o}C for 24 Hrs. Methanol was removed using rotary vacuum distillation to obtain faint yellow oily liquid. The produced amine ester monomer can be designated as octahydroxyethylamino pentaertheritoltetrapropanoate (OATP).

b) Synthesis of branched ionic liquid monomer (OATPS)

Equal mol amounts of OATP and PTSA were mixed in a flask equipped with a magnetic stirrer, thermometer and reflux condenser. The reaction temperature increased up to 145 ^{o}C and maintained for 24 h under nitrogen atmosphere. Finally, the viscous product of quaternized OSTP was obtained after cooling to room temperature.

c)Synthesis of magnetite capped OATPS

The $Fe^{3+}$and Fe^{2+} cations were produced from reaction of aqueous solutions $FeCl_3 \cdot 6H_2O$ with KI with molar ratio 3:1 under nitrogen atmosphere [**20**]. The produced $Fe^{3+}$and Fe^{2+} cations aqueous solution was stirred vigorously in the presence of equivalent mol ratios of OATPS ionic liquid and heated at 80◦C under nitrogen atmsphere. NH_4OH was added dropwise until the pH of solution reached 10. The black dispersed colloid solution of magnetite was produced after the reaction mixture heated and stirred to 90◦ for another 60 min to ensure complete growth of the magnetite nanoparticles. The black precipitates were collected after ultra- centrifuge the dispersed solution at 9000 rpm. The precipitate washed with water and ethanol until pH of solution reached pH 7 to remove unreacted chemical and then dried at 40◦C for 24 h. The reaction yield of magnetite capped with OATPS was 97.01 %.

2.3 Characterization:

Chemical structure of ionic liquid is confirmed using ^{1}H- and ^{13}CNMR spectra on a 400MHz Bruker Avance DRX-400 spectrometer.

X-ray diffraction (XRD) (Siemens D5000 using Cu K α irradiation) was used to investigate the crystal size and structure of the prepared magnetite nanoparticles.

The morphology of nanoparticles was investigated using a High Resolution Transmission Electron Microscope (HRTEM JEOL JEM-2100 F has acceleration voltage of 200 kV).

The particle size distribution and diameters of magnetite nanoparticles were evaluated by using Laser Zeta meter Malvern Instruments (Model Zetasizer 2000).

The surface activity and contact angles and surface tension measurements were determined using drop shape analyzer model DSA-100 at 25 ^{o}C.

The microstructure of steel was examined by a scanning electron microscope (SEM; Model JEOL-JSM-6300) and the chemical composition was estimated by electron dispersive X-ray (EDX) before and after immersion in 1M HCl in the presence and absence of OATPS inhibitor.

2.4 Electrochemicl measurements

Electrochemical experiments were performed using a potentiostat/galvanostat Solartron 1470E system. Polarization curves were carried out with a scan rate of 1mV/s after 1 h immersion in 1M HCl (uninhibited solution) and inhibited solutions. EIS data were conducted over a frequency range from 10KHz to 10 mHz. All electrochemical data were collected and analyzed using software package developed by Scribner Associates, Inc (UK)

3. Results and discussion

3.1. Chemical structure of branched OATPS IL

The present work aims to create a new class of branched electrolytes to use as thin anticorrosive layer film for steel. In the previous work [31], hyperbranched polymer produced from modification of pentaerytheritol tetraacrylate (PETA) by reaction with diethanolamine (DEA) via Michael addition reaction of the vinyl group to the secondary amine groups to produce octahydroxyethylamino pentaertheritoltetrapropanoate (OATP). The present work used PTSA to quaternize OATPS product as illustrated in the Scheme 1. The modification was used to prepare water soluble hyperbranched ionic liquid polymer. It is expected that the more branches the dendritic polymer has, the more effective it is in anticorrosive protection performance.

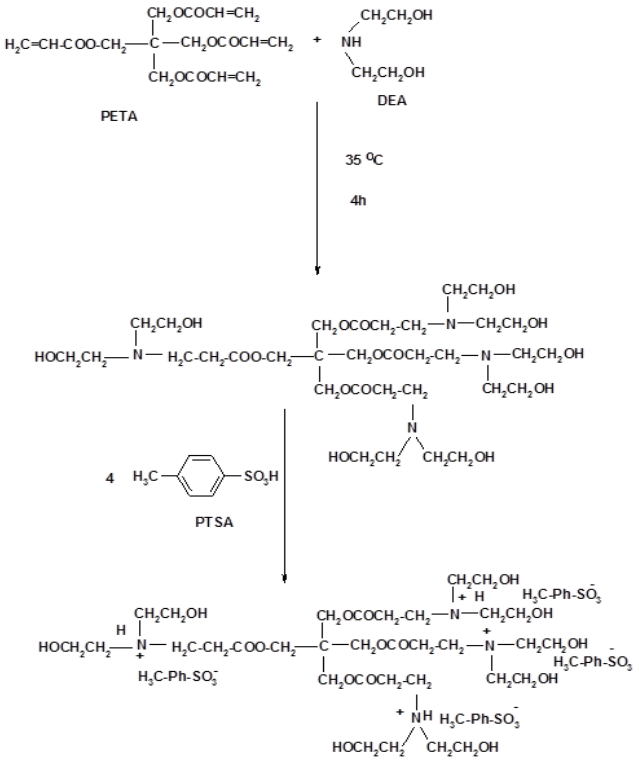

Scheme 1: Synthesis of branched OATPS IL.

The molecular structure of the OATP was confirmed by ^{1}H and ^{13}C NMR spectroscopy which represented in Figures 1 and 2. It can be noticed from ^{1}H NMR that there are four new peaks at 7.64 and 7.30 ppm (doublet of doublet), 4.1 (broad heptet), and 2.37 ppm (singlet) which attributed to phenyl protons, NH salt and methyl attached to phenyl group of PTSA, respectively. These peaks indicated the quaternization of OATP with PTSA. The disappearance of peaks at 5.59 and 6.07 which attributed to vinyl protons of PETA and appearance of new peaks at 2.8 ppm (attributed to (COCH2-CH2-N (–OCOCH2CH2–), 2.88 ppm (–$OCOCH_2$) indicated that Michael addition occurred between DEA and PETA. Moreover, the peaks at 3.5–3.8 (–$N(CH_2CH_2O)_2$ and 3.4 ppm (-OH) indicated that the presence of DEA in the chemical structure of OATPS.

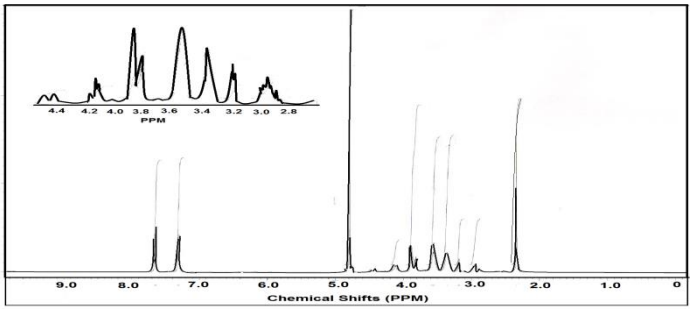

Fig 1: ^{1}HNMR spectrum of quaternized OATPS with PTSA.

Another evidence for chemical structure of OATP was confirmed by ^{13}CNMR data (Figure 2). The appearance of peaks at 144, 133, 129, 127 and 21 ppm which attributed to phenyl and methyl carbons indicated the incorporation of PTSA in the chemical structure of OATP. The presence of peaks at 28, 49, 55, 57 and 172.2 ppm which attributed to C-(OCO)4, CH_2OH,

CH_2CH_2O, CH_2CH_2N and COO, respectively. The data indicated that the chemical structure of OATP product as illustrated in Scheme 1.

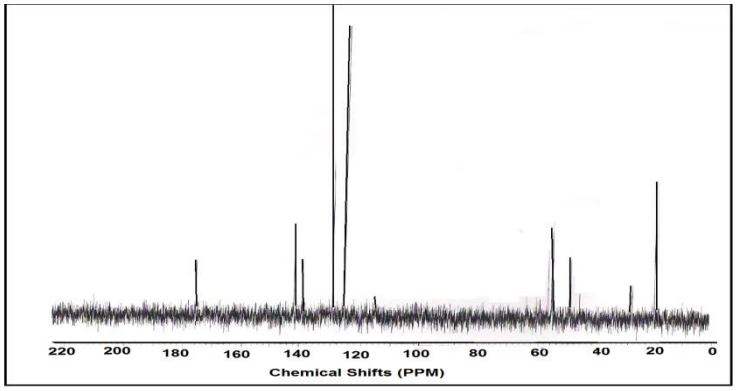

Fig. 2: ^{13}CNMR spectrum of quaternized OATP with PTSAS.

3.2. Preparation of magnetite capped nanoparticles with OATPS

There are different methods have been used to prepare magnetite nanoparticles such as hydrothermal, thermal decomposition, forced hydrolysis, electrochemical synthesis, sono-chemical method and ultrasonic assisted impregnation [32-34]. The co-precipitation method succeeded to prepare magnetite with high yields ranged from 96 to 99.9 % [20]. The magnetite nanoparticles have great tendency to form aggregates or to oxidized to other oxides beside low stability to acids when they were not protected by suitable capping agents. In this work, we aim to prepare magnetite capped with prepared IL as illustrated in Scheme 2. The electrostatic and steric "electrosteric" properties of IL can stabilize MNPs as described in scheme 2. The stabilization of magnetite by IL can be referred to the ionic nature, polarity and super molecular network (scheme 2) of IL that surrounded the magnetite nanoparticles [35-38]. The hydrogen bonds between cations and anions of IL molecules form network assists in the stabilization of magnetite nanoparticles [35-37]. The combination of undirected Coulomb forces and directed hydrogen bonds forms network with super molecular structure that assists the formation of capped magnetite nanoparticles. The IL network will form well define magnetite nanoparticles capped with OATPS.

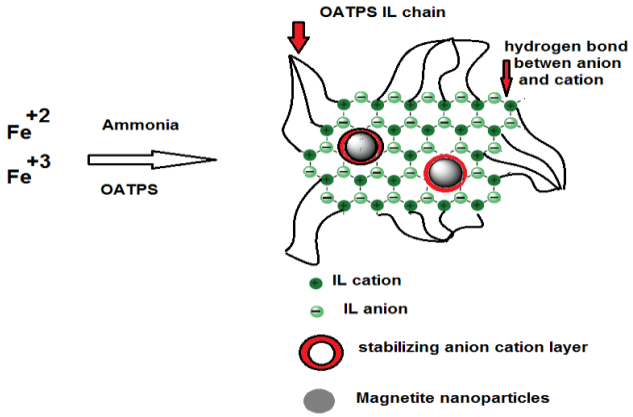

Scheme 2: Synthesis of magnetite capped nanoparticles with OATPS.

The morphology of the prepared magnetite nanoparticles capped with OATPS was investigated by HR-TEM as illustrated in Figure 3. The micrographs indicated that monodisperse magnetite nanoparticles with uniform structure were formed due to the presence of OATPS as IL which prevents the agglomeration of magnetite. The magnetite nanoparticles was appeared as

black dots inside the nanoparticles. The presence of OATPS can be indicated from the transparent layer that surrounded the black dots as confirmed from Figure 3.

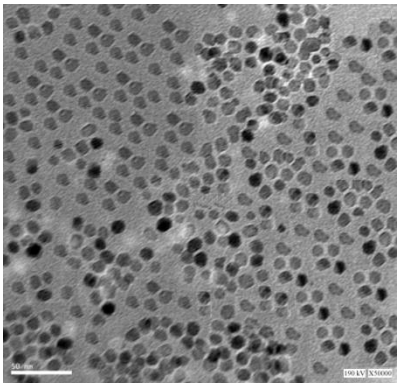

Fig. 3: TEM micrograph of magnetite capped nanoparticles with OATPS.

The high mono disperseability of magnetite capped nanoparticles with OATPS and the particle size were confirmed from Zeta size measurements as represented in Figure 4. The data indicated that the particle size was 12.8 nm and the polydispersity index was 0.0103. These data agree with the TEM results and confirm the presence of branched ionic liquid based on OATPS will form stable and uniform magnetite polar nanoparticles.

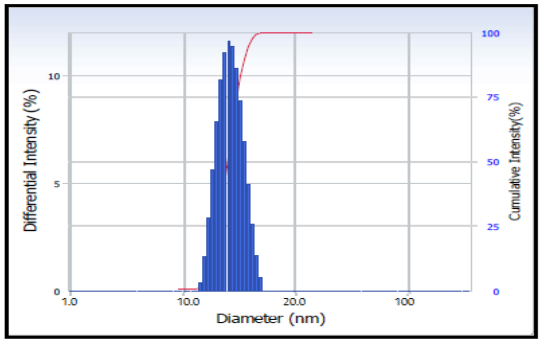

Fig. 4: Particle diameter and disperse index of magnetite capped nanoparticles with OATPS.

The crystal structure of magnetite capped nanoparticles with OATPS and their spilliting pattern were confirmed from XRD analysis as illustrated in Figure 5. The data diffractogram (Figure 5) indicates the plans of magnetite as compared with JCPDS Card No. (79 - 0417). The appearance of same diffraction peaks at the same 2-theta values confirms that pure magnetite was firmed without the presence of other iron oxide impurities.

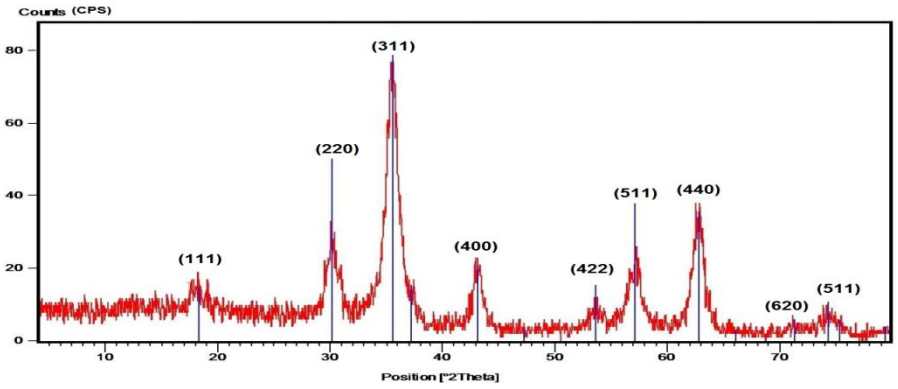

Fig. 5: XRD diffractograms of magnetite capped nanoparticles with OATPS.

The wettability of steel with water and corrosive environment is one of the most effective parameters that affect the corrosion of steel [39]. The contact angle (θ) formed between corrosive media and steel is a good indicator for the interaction between the steel and corrosive environments. In this respect, the contact angles of bare steel with water, 1M HCl aqueous solution are represented in Figure 6. and indicated that there is a good interaction between the steel surfaces and branched OATPS inhibitor. The obtained data proved the adsorption of the inhibitor on the metal surface [40]. It is clear that in all cases, the great reduction of contact angles in the presence of magnetite capped nanoparticles with OATPS confirming the suggestion that the prepared magnetite capped nanoparticles with OATPS used is more highly adsorbed and adhered on the steel surfaces and can be used to form thin film layer on the metal surfaces in acid medium. Figure 6 displays the contact angle, θ, as a function of magnetite capped nanoparticles with OATPS concentration for acid solutions on mild steel. It was noticed that the θ values were increased with increment of magnetite capped nanoparticles with OATPS concentration. The increment of contact angle data indicates the formation of hydrophobic films that inhibit the diffusion of acid on the steel surfaces. These data agree in harmony with the data reported before for increasing of contact angles of metal surface with increment corrosion inhibitor concentrations [41]. The obtained results of θ in water, 1M HCl and 100 ppm of branched OATP are 104, 77 and 42°, respectively. Therefore it was concluded that the presence of OATPS as thin layer produces hydrophobic steel surface[42].

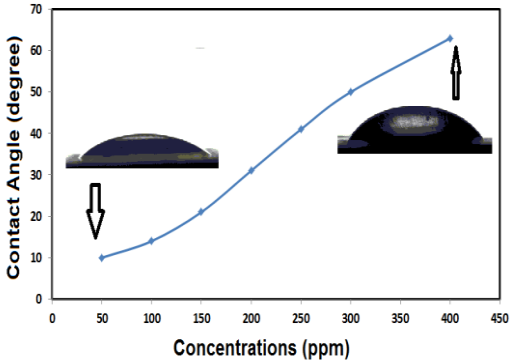

Fig. 6: Contact angle of 1M HCl solutions containing different concentrations of OATPS ionic liquid on mild steel surface.

3.3. Potentiodynamic Polarization Measurements

The data of cathodic and anodic polarization curves for steel electrode in the absence and presence of OATPS IL or magnetite capped nanoparticles with OATPS are shown in Figures 7 and 8. It is can be seen that the presence of magnetite capped nanoparticles with OATPS lowered the

current densities of both anodic and cathodic curves and the decrease of the corresponding current densities was more pronounced at lower concentrations more than the OATPS IL concentration. The results may be attributed to the adsorption of magnetite capped nanoparticles with OATPS more than OATPS IL on the steel surface [43].The adsorption of OATPS IL on the steel surface causes a suppression of the cathodic and anodic processes via blocking the available reaction sites [44]. The surface coverage of steel increases with increasing magnetite capped nanoparticles with OATPS concentration by more adsorption of the magnetite capped nanoparticles with OATPS and formation of barrier layer, which reduces the diffusion of the aggressive ions . This will provide protection to steel against corrosion [45]. All the calculated electrochemical parameters are given in Tables 1 and 2.

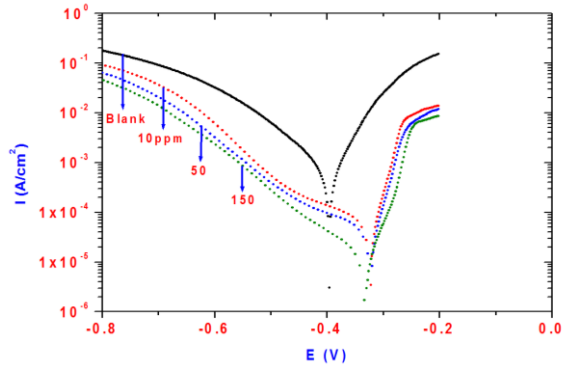

Fig. 7. Effect of OATPS IL concentration on Polarization curves for steel in 1M HCl

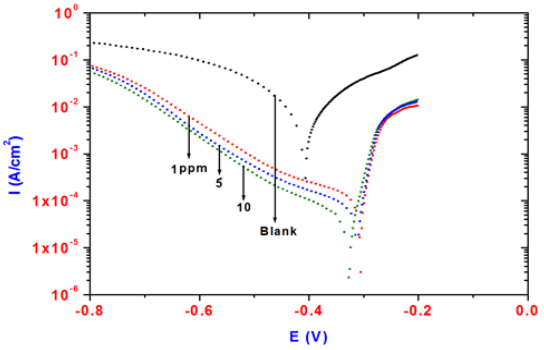

Figure 8 . Polarization curves for steel in 1.0 M HCl containing different concentrations of magnetite capped nanoparticles with OATPS.

Table 1. Inhibition efficiency values for steel in 1M HCl with different concentrations of ERIT-PEG Surfactant calculated by Polarization and EIS methods.

	Polarization Method					EIS Method		
	Ba (mV)	Bc (mV)	E_{corr} (V)	i_{corr} µA/cm^2	IE%	R_{ct} Ohm	Cdl (µF/cm^2)	IE%
Blank	69	120	-0.3955	839	_____	1.80	334	____
10ppm	47	237	-0.3233	69	91.7	21	106	91.1
50	46	270	-0.3225	54	93.5	35	103	94.8
150	43	137	-0.3315	14	98.3	90	91.0	98.0

Table 2. Inhibition efficiency values for steel in 1M HCl with different concentrations of magnetite capped nanoparticles with OATPS calculated by Polarization and EIS methods

	Polarization Method					EIS Method		
	Ba (mV)	Bc (mV)	E_{corr} (V)	i_{corr} µA/cm^2	IE%	R_p Ohm	Cdl (µF/cm^2)	IE%
Blank	69	120	-0.3955	839	_____	1.80	334	____
1ppm	50	394	-0.3061	152	81.8	10.1	137	82.1
5	41	173	-0.3139	49	94.1	35	106	94.8
10	46	195	-0.3282	44	94.7	36	104	95.0

The shift in Ecorr with in presence magnetite capped nanoparticles with OATPS towards more positive values indicating that OATPS IL plays a strong role in suppressing the anodic reaction. The presence magnetite capped nanoparticles with OATPS concentration confirms the higher the protection performance of the inhibitor. It can be concluded that that the OATPS IL and magnetite capped nanoparticles with OATPS can be labeled as a mixed-type inhibitor with predominant anodic effect. The values of the corrosion current density in the uninhibited and inhibited solution were used to estimate the inhibition efficiency (IE%) as follows [46]:

$$IE\% = [\, 1 - (i_{corr\,(inh)} / i_{corr\,(uninh)})] \times 100 \qquad (1)$$

where $i_{corr(uninh)}$ and $i_{cor(inh)}$ are corrosion current density values in the uninhibited and inhibited solution, respectively. It is clear that the IE values increased with increasing concentration of the inhibitor, and the maximum IE value was 98% and 95 % at 150 and 10 ppm of OATPS IL and magnetite capped nanoparticles with OATPS, respectively . The result can be attributed to the formation of insulating film on the steel surface, which suppresses the corrosion process. The data of (IE%) presented in Tables 1and 2 indicated that magnetite capped nanoparticles with OATPS had good protection performance even at low concentrations. The higher the OATPS IL concentration indicates the better the protection of steel. The results can be explained on the basis of more diminishing of the corrosion current density with increasing OATPS IL and magnetite capped nanoparticles with OATPS concentrations.

The Nyquist plots of steel obtained in 1 M HCL solution with various concentrations of OATPS IL and magnetite capped nanoparticles with OATPS are shown in Figure 9 and 10. It is evident that the Nyquist plot for steel in the test solution consists of a capacitive loop. The inhibited solution has bigger size of impedance plots than that experienced by uninhibited one. The presence of OATPS IL and magnetite capped nanoparticles with OATPS led to an increase in the diameter of capacitive loop.

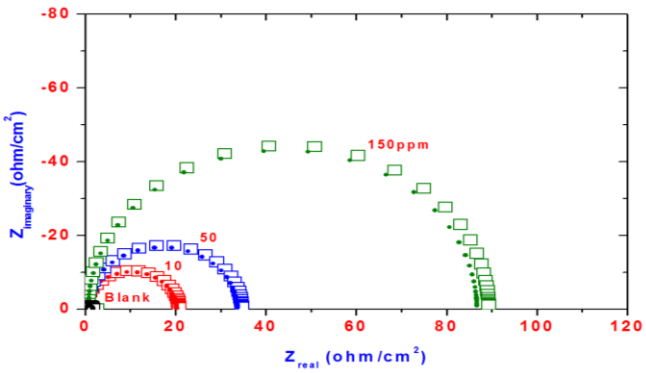

Fig. 9. Effect of OATPS IL concentration on Nyquist diagrams for steel in 1M HCl solution.

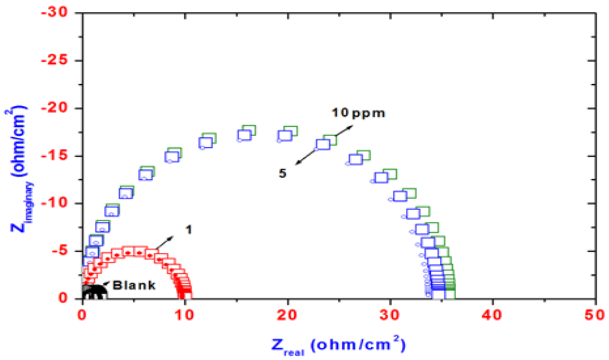

Fig. 10 . Nyqusit plot for steel in 1.0 M HCl containing different concentrations of magnetite capped nanoparticles with OATPS.

The experimental data was fitted by an equivalent circuit consists of the series connection of a solution resistance (Rs) with a parallel connection of a charge transfer resistance (Rct) and a double layer capacitance (Cdl) . The values of Rct and Cdl obtained from fitting the EIS data are quoted in Tables 1 and 2. It is evident that the values of Rct increase while Cdl decrease within the investigated concentration range. The adsorption of OATPS IL and magnetite capped nanoparticles with OATPS with a formation of an insulating and inhibitive film led to an increase in the in Rct values. This layer acts as barrier for diffusion of the aggressive ions and hindered the steel surface from attacking with the chloride ions [47]. The decrease in the local dielectric constant of the protective layer in the inhibited solution can be accounted to the replacement of water molecules of high dielectric constant with OATPS IL and magnetite capped nanoparticles with OATPS molecules with low dielectric constant. The higher the amount of absorbed OATPS IL molecules on the steel surface confirms the thicker the formed barrier layer on steel surface [48]. The inhibition efficiency (IE%) is calculated from the Rct values using the following formula [49]:

$$IE\% = [1- (R^1_{ct}/R^2_{ct})] \times 100 \quad (2)$$

Where R^1_{ct}, and R^2_{ct} were referred the charge transfer resistances in the uninhibited and inhibited solution , respectively. The estimated values of IE% at different OATPS IL and magnetite capped nanoparticles with OATPS concentrations are quoted in Tables 1 and 2. The surface coverage of steel surface increased with increasing the OATPS IL concentrations, which led to an increase in the protection performance of the investigated inhibitor.

The formation of protective film on the steel surface by using is examined by SEM and EDX analyses as illustrated in Figure 7. The steel coupon was immersed in 10 ppm solution of magnetite capped nanoparticles with OATPS for 2 h and dried in air as represented in Figure 11a. The produced films were immersed in 1M HCl solution for 24 h as illustrated in Figure 11c. The EDX analyses of steel immersed in 1M HCl and that coated with 100 ppm of magnetite capped nanoparticles with OATPS are represented in Figure 11 b and d, respectively.

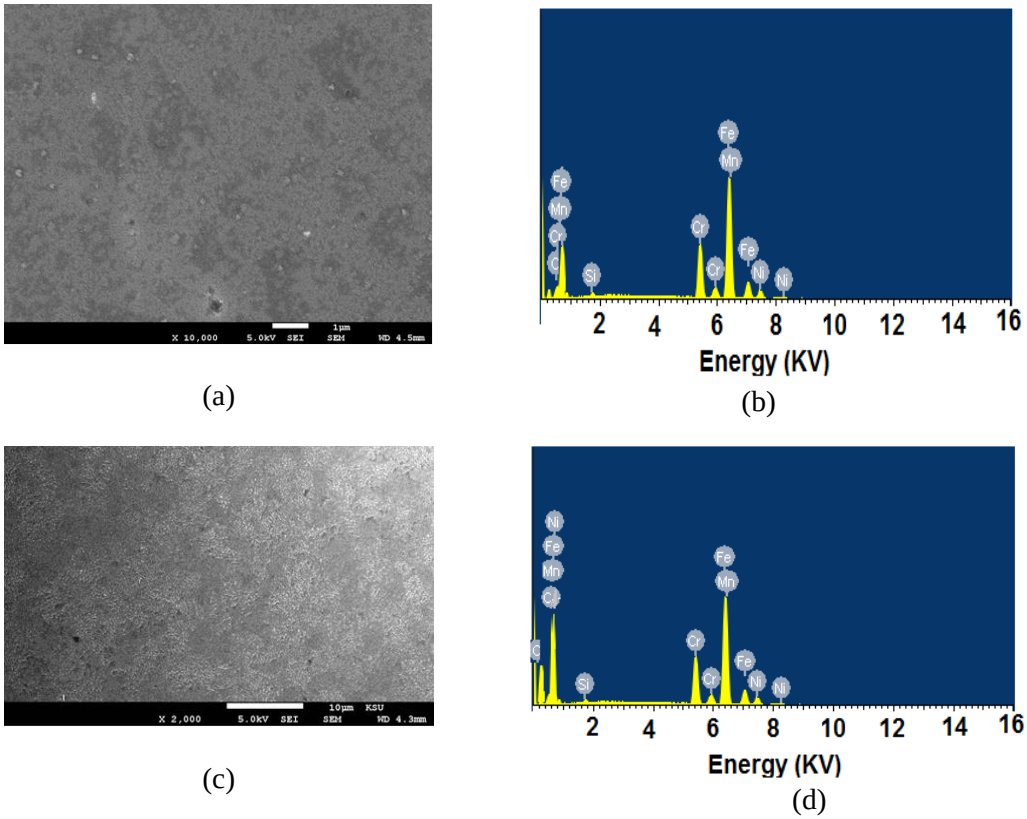

Fig. 7: SEM and EDX analyses of steel a) immersed in 10 ppm of magnetite capped nanoparticles with OATPS, b) immersed in 1M HCl absence of inhibitor, c) and d) immersed in 1M HCl in the presence 100 ppm of OATPS.

The SEM micrographs indicate that protective films are formed on the steel surface and the surface remained almost free from any corrosion products. This was referred to the formation of assembled film as highly stable and protective against the attack of aggressive corrosive environment. The mechanism of film formation can be referred to the electrostatic interactions and charge differences that obtained between charged ionic liquid OATPS and steel surface. It is expected to promote crystal growth of magnetite capped nanoparticles with OATPS to produce smoother adherent deposit as illustrated in Figure 11. This was reinforced by EDX analyses, Figure 11 b and d, that produced two new signals produced for Fe and oxygen to produce Fe_2O_3 film. The presence of inhibitor (Figure 11d) increased the carbon and oxygen content that indicate the presence of organic films as protective layer.

4. Conclusions

The magnetite capped nanoparticles with OATPS was prepared with high disperability and uniform particle size were prepared in the presence of new IL. The Electrochemical results revealed that OATPS IL effectively inhibited the steel corrosion in acidic media. Polarization data indicated that magnetite capped nanoparticles with OATPS suppresses the anodic and cathodic reactions and behaves as mixed type inhibitors. The EIS results revealed that the OATPS IL functioned via adsorption of the magnetite capped nanoparticles with OATPS on the steel/solution interface.The protection corrosion performance of magnetite capped nanoparticles with OATPS increased at 10 ppm low concentration.

Acknowledgment

The authors extend their appreciation to the Deanship of Scientific Research at King Saud University for funding this work through research group no RGP- 235.

References

[1] M. Finšgar, J. Jackson, Corros. Sci. **86,** 171(2014).
[2] T. Gu, Z. Chen, X. Jiang, L. Zhou, Y. Liao, M. Duan, H. Wang, Q. Pu, Corros. Sci. **90,** 118 (2015).
[3] Q.B. Zhang, Y.X. Hua, Electrochimica Acta **54,** 1881(2009).
[4] C. A. Flores, E. A. Flores, E. Hernández, L.V. Castro, A. García, F.Alvarez, F. S. Vázquez, Journal of Molecular Liquids **196,** 249(2014).
[5] J. Łuczak, J. Hupka, J. Thoming, C. Jungnickel, Colloids and Surfaces A:Physicochem. Eng Aspects **329,** 125(2008).
[6] M.L. Free, Corros. Sci. **44,** 2865(2002).
[7] P. Li, J.Y. Liqb, K.L. Tanb, J.Y. Leea, Electrochim. Acta **42,** 605(1997).
[8] Q.B. Zhang, Y.X. Hua, Electrochim. Acta **54**, 1881(2009).
[9] Z. Peng, Z. Cheng, H. Lei, N. Lihong, Z. Fushi, Corros. Sci. **50,** 2166(2008).
[10] H. Ashassi-Sorkhabi, M. Es'haghi, Mater. Chem. Phys. **114,** 267(2009).
[11] V.V. Shevchenko, A.V. Stryutsky, N.S. Klymenko, M.A. Gumenna, A.A. Fomenko, V.N. Bliznyuk, V.V. Trachevsky, V.V. Davydenko, V.V. Tsukruk, Polymer **55,** 3349(2014).
[12] J. Yuan, M.Antonietti, Polymer **52,** 1469(2011).
[13] J. Yuan, D. Mecerreyes, M.Antonietti, Prog Polym Sci. **38,** 1009(2013).
[14] M. Okazaki, L. Washio, Y. Shibasaki, M. Ueda, J. Am. Chem. Soc. **125,** 8120(2003).
[15] F. Gröhn, B.J. Bauer, E.J. Amis, Macromolecules **34,** 6701(2001).
[16] J.F.G.A. Jansen, E.M.M. de Brabander-Van den Berg, E.W. Meijer, Science **266**, 1226 (1994).
[17] A. M. Atta, O. E. El-Azabawy, H.S. Ismail, M. Hegazy Corr. Sci. 53, 1680 (2011).
[18] M. A. Akl, A. M. Atta, A. M. Yousef, M. I .Alaa, Polym Int **62**, 1667 (2013).
[19] A. M. Atta, G. A. El-Mahdy, H. A. Al-Lohedan, , Digest Journal of Nanomaterials and Biostructures **9**, 627 (2014).
[20] A. M. Atta , G. A. El-Mahdy, H. A. Al-Lohedan, S. A. Al-Hussain, Int. J. Mol. Sci. **15**, 6974 (2015).
[21] J. Dupont, J.D. Scholten, Chem Soc Rev, **39**,1780 (2010).
[22] P. Migowski, J. Dupont, Chem Eur J **13**, 32 (2007).
[23] K. Ho, W. Li, C. Wong, P. Li, Colloid Polym Sci **288**:1503 (2010).
[24] J. Amici, M. Sangermano, E. Celasco, Y. Yagci. Eur Polym J **47**,1250 (2011).
[25] J. Yuan, S. Wunder, F. Warmuth, Y. Lu, Polymer;**53**: 43 (2012)
[26] R. Marcilla, M.L. Curri, P.D. Cozzoli, M.T. Martnez, I . Loinaz, Small **2**, 507 (2006).
[27] Y. Peng, X. Wu, L. Qiu, C. Liu, S. Wang, F.Yan, J Mater Chem **1**, 9257 (2013).
[28] A.M. Atta, G.A. El-Mahdy, H.A. Allohedan, M.M.S. Abdullah, Int. J. Electrochem. Sci **10**, 6106 (2015).
[29] G.A. El-Mahdy, A.M. Atta, H.A. Al-Lohedan, A.O. Ezzat, Int. J. Electrochem. Sci **10**, 5812 (2015).
[30] A. M. Atta, · G. M. El-Mahdy, · H. A. Allohedan, ·M.M. S. Abdullah, Int. J. Electrochem. Sci., **11**, 882 (2016) .
[31] G. A. El-Mahdy, A.M. Atta, H. A. Al-lohedan, A.O. Ezzat, Int. J. Electrochem. Sci. **9**, 7925 (2014).
[32] L. Cabrera, S. Gutierrez, N. Menendez, M.P. Morales, P. Herrasti, Electrochim.Acta **53**, 3436 (2008).
[33] P. Loekitowati Hariani, M. Faizal, R. Ridwan, M. Marsi, D. Setiabudidaya, Int. J. Environ. Sustain. Dev. **4**, 336 (2013).
[34] D. Maity, S.N. Kale, R. Kaul-Ghanekar, J.-M. Xue, J. Ding, J. Magn. Magn. Mater.

321, 3093 (2009).
[35] J. Kr¨amer, E. Redel, R. Thomann, C. Janiak, Organometallics **27**, 1976 (2008).
[36] K. Ueno, H. Tokuda, M. Watanabe, Phys. Chem. Chem. Phys. **12**, 1649 (2010).
[37] M.-A. Neouze, J. Mater. Chem. **20**, 9593 (2010).
[38] C. S. Consorti, P. A. Z. Suarez, R. F. de Souza, R. A. Burrow, D. H. Farrar, A. J. Lough, W. Loh, L. H. M. da Silva, J. Dupont, J. Phys. Chem. B **109**,4341 (2005).
[39] M. Mantel and J.P. Wightman, Surface & Interface Analysis **21**, 595(1994).
[40] T. Zhao, G. Mu, Corros. Sci. **41**, 1937 (1999).
[41] A. K. Singh, E. E. Ebenso, M. A. Quraishi, Int. J. Electrochem. Sci. **7**, 2320 (2012).
[42] S. Ashhari, A. A.Sarabi, Surf. Interface Anal. (2014). (wileyonlinelibrary.com) DOI 10.1002/sia.5706.
[43] G. Quartarone, M. Battilana, L. Bonaldo, T. Tortato, Corros. Sci.**50**, 3467 (2008).
[44] E. E. Ebenso, T, Arslan, F. Kandemirli, N. Caner, N. I. Love, Int. J. Quantum Chem. **110,** 1003 (2010).
[45] T. Arslan, F. Kandemirli, E. E. Ebenso, I. I. Love, Corros. Sci. **51**, 35 (2009).
[46] Q. Qu, L. Li, W. Bai, S. Jiang, Z. Ding, Corros. Sci. **51**, 2423 (2009) .
[47] S. Murlidharan, K. L. N. Phani, S. Pitchumani, S. Ravichandran, Polyamino. J. Elecrrochem.Soc. **142**. 1478 (1995) .
[48] K. Babić-Samardžija, C. Lupu, N. Hackerman, A.R. Barron, A. Luttge, Langmuir **21**, 12187(2005) .
[49] Z. Tao, W. He, S. Wang, S. Zhang, G. Zhou, Corros. Sci. **60**, 205 (2012).